Cell Reports Medicine, Volume *4*

Supplemental information

The Fc-effector function of COVID-19 convalescent plasma contributes to SARS-CoV-2 treatment efficacy in mice

Irfan Ullah, Guillaume Beaudoin-Bussières, Kelly Symmes, Marc Cloutier, Eric Ducas, Alexandra Tauzin, Annemarie Laumaea, Michael W. Grunst, Katrina Dionne, Jonathan Richard, Philippe Bégin, Walther Mothes, Priti Kumar, Renée Bazin, Andrés Finzi, and Pradeep D. Uchil

Figure S1

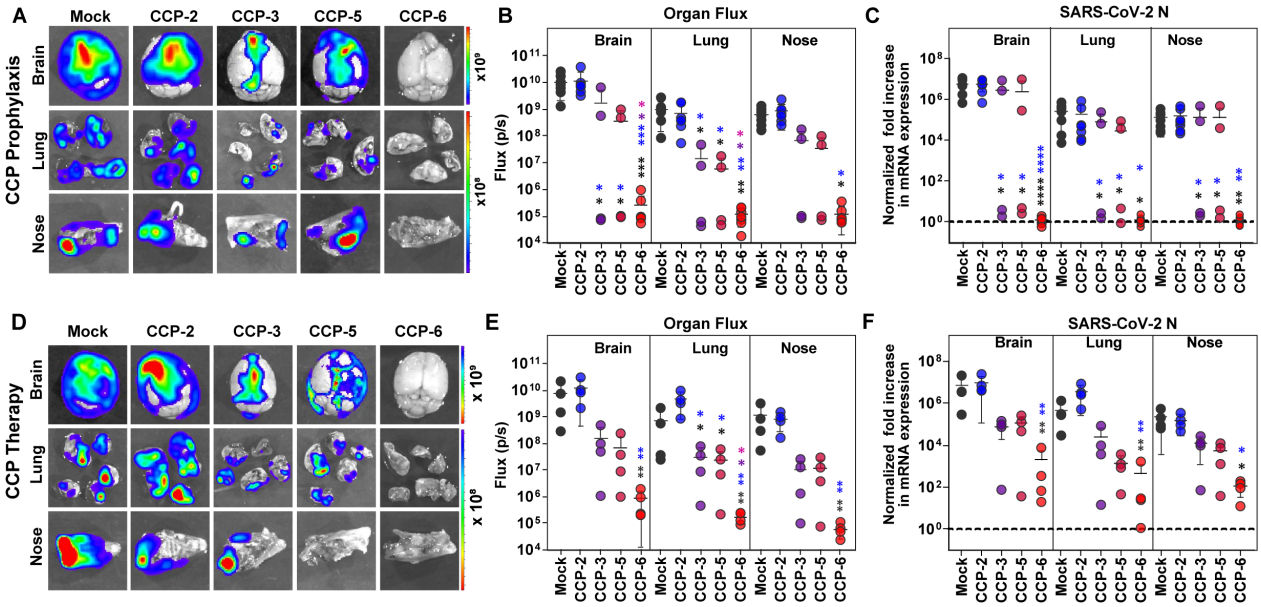

Figure S1. CCP Efficacy During Prophylaxis and Therapy in K18-hACE2 Mice Against Lethal SARS-CoV-2 Challenge. Related to Figure 1 and 2

(A-E, F-G, and I-J) *Ex vivo* imaging of indicated organs and quantification of nLuc signal as flux(photons/sec) after necropsy for an experiment shown in Figure 1B (CCP prophylaxis) and Figure 2A (CCP therapy)

(H, K) Fold change in SARS-CoV-2 nucleocapsid (N gene) expression in brain, lung and nose tissues for experiment as in Figure 1B and 2A. The data were normalized to *GAPDH* mRNA expression in the same sample and that in non-infected mice after necropsy.

Post necropsy analyses were determined after necropsy for mice that succumb to infection at 6 dpi and for surviving mice at 16 dpi (CCP prophylaxis) or 18 dpi (CCP therapy).

Grouped data in (G, H) and (J, K) were analyzed by 2-way ANOVA followed by Tukey's multiple comparison tests. Statistical significance for group comparisons to isotype are shown in black, with CCP-2 are shown in blue, CCP-3 are shown in purple and with CCP-5 are shown in light red. ∗, $p < 0.05$; ∗∗, $p < 0.01$; ∗∗∗, $p < 0.001$; ∗∗∗∗, $p < 0.0001$; Mean values ± SD are depicted.

Figure S2

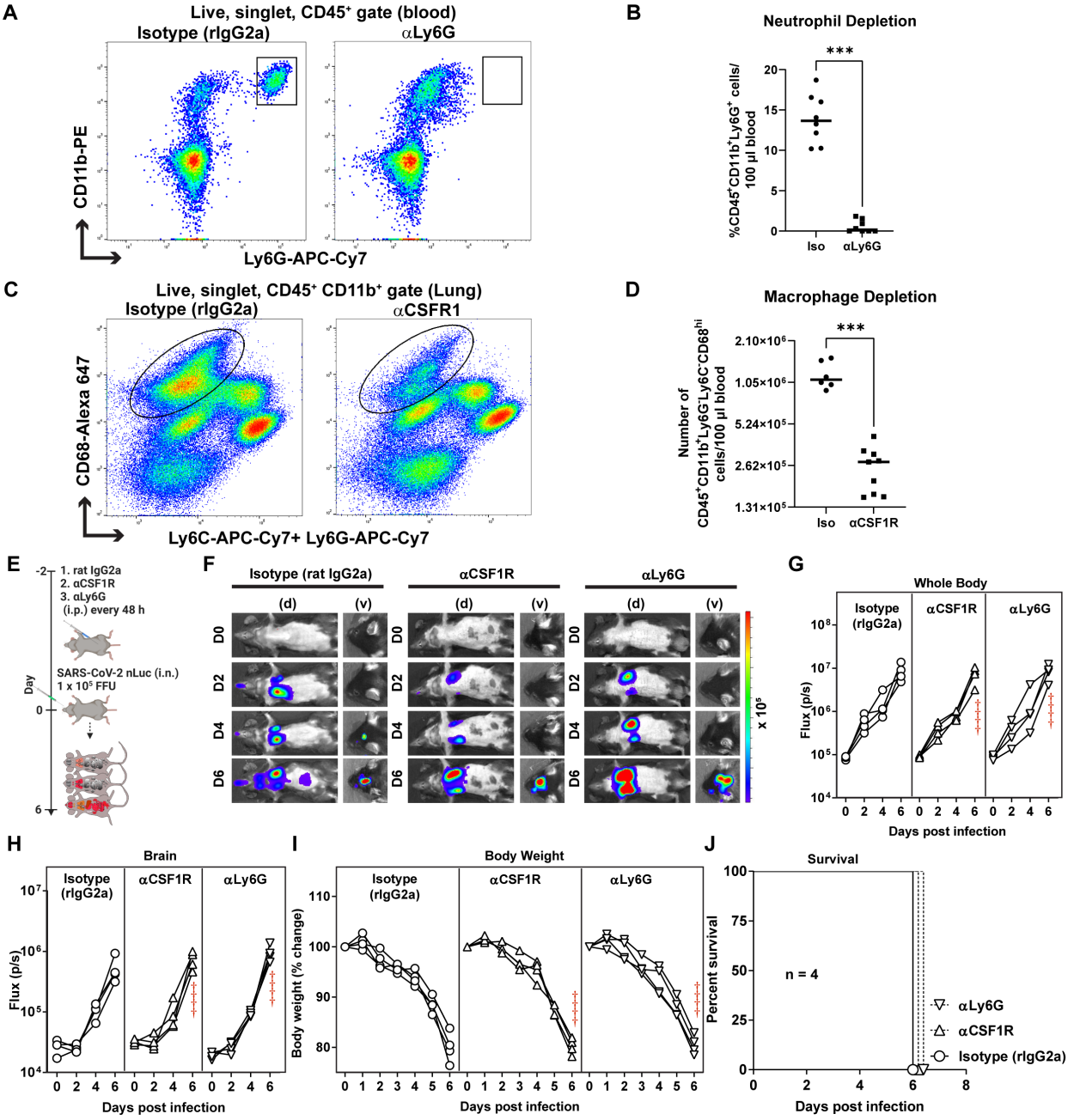

Figure S2. Immuno-depletion of Neutrophils and Macrophages does not Influence SARS-CoV-2 Replication in K18-hACE2 Mice. Related to Figure 3

(A, B) Representative FACS plots showing the gating strategy to identify neutrophils ($CD45^+CD11b^+Ly6G^+$) (n= 8; two experiments) and quantification to ascertain their depletion in blood of indicated groups of mice.

(C, D) Representative FACS plots showing the gating strategy to identify tissue resident macrophages in lungs ($CD45^+$ $CD11b^+Ly6G^-Ly6C^-CD68^+$) (n=8; two experiments) and quantification to ascertain their depletion in single cell suspensions of lung tissue in indicated groups of mice.

(B, D): Non-parametric Mann-Whitney test; ∗, $p < 0.05$; ∗∗, $p < 0.01$; ∗∗∗, $p < 0.001$; ∗∗∗∗, $p < 0.0001$; Mean values ± SD are depicted.
(E) Experimental design to test effect of macrophages ($CD45^+Ly6G^-Ly6C^-CD11b^+CD68^+$) and neutrophils ($CD45^+CD11b^+Ly6G^+$) depletion in K18-hACE2 mice challenged with SARS-CoV-2-nLuc (1×10^5 FFU). αCSFR-1 or αLy6G mAbs (i.p., 20 mg/kg body weight) were used to deplete macrophages or neutrophils respectively every 48h starting at -2 dpi. Rat isotype mAb treated cohorts served as controls (Iso). Animals were followed by non-invasive BLI every 2 days as indicated.
(F) Representative BLI images of SARS-CoV-2-nLuc-infected mice in ventral (v) and dorsal (d) positions for experiment as in E. Scale bars denote radiance (photons/sec/cm^2/steradian).
(G, H) Temporal quantification of nLuc signal as flux (photons/sec) computed non-invasively.
(I) Temporal changes in mouse body weight with initial body weight set to 100% for an experiment shown in E.
(J) Kaplan-Meier survival curves of mice (n = 4 per group; two experiments) for experiment as in E.

Figure S3

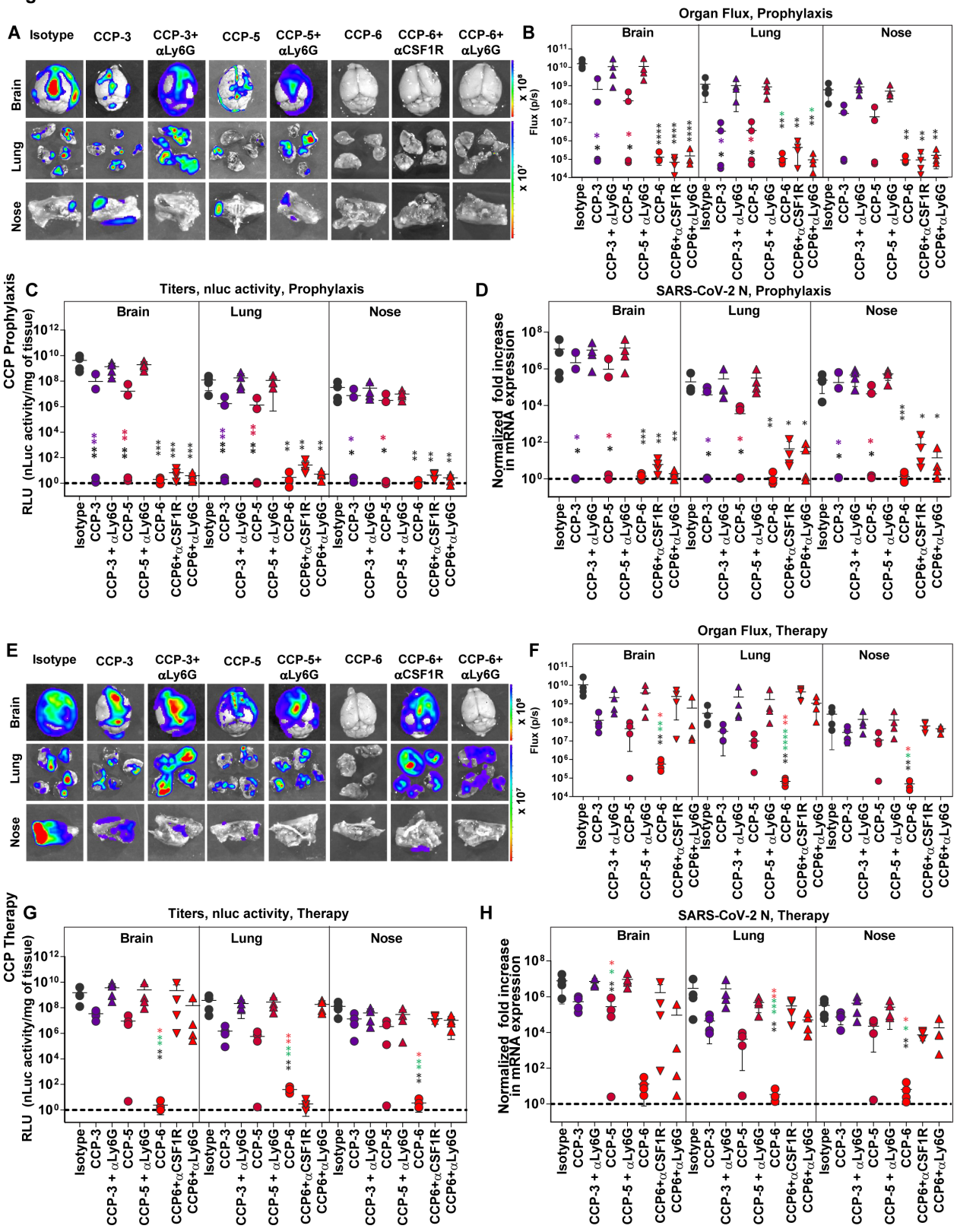
A
Isotype
CCP-3
CCP-3+ αLy6G
CCP-5
CCP-5+ αLy6G
CCP-6
CCP-6+ αCSF1R
CCP-6+ αLy6G
Brain
Lung
Nose
x 10⁸
x 10⁷
B
Organ Flux, Prophylaxis
Flux (p/s)
C
Titers, nluc activity, Prophylaxis
CCP Prophylaxis
RLU (nLuc activity/mg of tissue)
D
SARS-CoV-2 N, Prophylaxis
Normalized fold increase in mRNA expression
E
F
Organ Flux, Therapy
G
Titers, nluc activity, Therapy
CCP Therapy
H
SARS-CoV-2 N, Therapy

Figure S3. Effect of Innate Immune Cell Depletion on CCP-mediated Protection during Prophylaxis and Therapy. Related to Figure 3 and 4

(A-B, E-F) *Ex vivo* imaging of indicated organs and quantification of nLuc signal as flux (photons/sec) after necropsy in K18-hACE2 mice for an experiment shown in Figure 3A (CCP-prophylaxis) and 4A (CCP-therapy).

(C, G) Viral loads (nLuc activity/mg) in indicated tissue and condition measured on Vero E6 cells as targets. Undetectable virus amounts were set to 1

(D, H) Fold change in SARS-CoV-2 nucleocapsid (N gene) expression under indicated conditions tissues. The data were normalized to *Gapdh* mRNA expression in the same sample and that in non-infected mice after necropsy.

Grouped data in (B-D) and (F-H), were analyzed by 2-way ANOVA followed by Tukey's multiple comparison tests. Statistical significance for group comparisons to isotype control are shown in black, with CCP-3 to CCP-3+αLy6G are shown in purple, with CCP-5 to CCP-5+αLy6G are shown in light red and CCP-6+αCSF1R are shown in green and with CCP-6 αLy6G are shown in red. $*$, $p < 0.05$; $**$, $p < 0.01$; $***$, $p < 0.001$; $****$, $p < 0.0001$; Mean values ± SD are depicted.

Figure S4

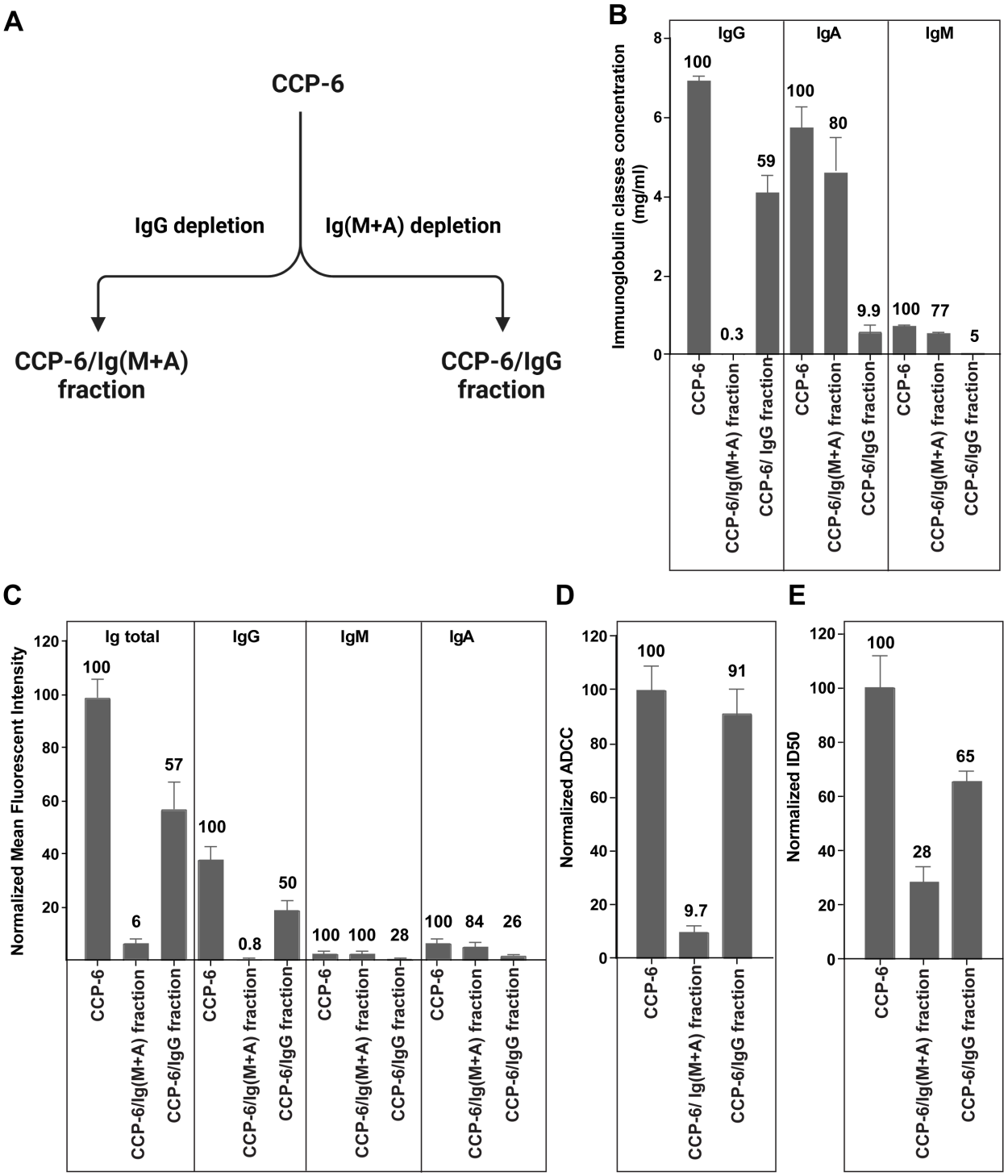

Figure S4. Characterization of class-depleted CCP-6. Related to Figure 5

(A) A scheme showing nomenclature of fractions after IgG or Ig(M+A) depletion of CCP-6.
(B) Evaluation of indicated Ig class concentration in complete and depleted CCP-6 using ELISA. The relative concentration (%) of each class in the different fractions is shown above the bars.

(C) Levels of Spike-specific denoted antibody classes in complete or depleted CCP-6 fractions, measured by flow cytometry.
(D) Normalized *in vitro* ADCC activity in complete and depleted CCP-6 fractions evaluated using CEM.NKr cells:CEM.NKr.Spike cells (1:1) as targets and PBMCs from an uninfected donor as effectors.
(E) *In vitro* neutralization of Spike-decorated lenti-pseudoviral particles by complete and depleted CCP-6 fractions.
Undepleted CCP-6 plasma was used for normalizations shown in (B-E) and set to 100%. Mean values ± SD from 3 experiments or replicates is depicted.

Figure S5

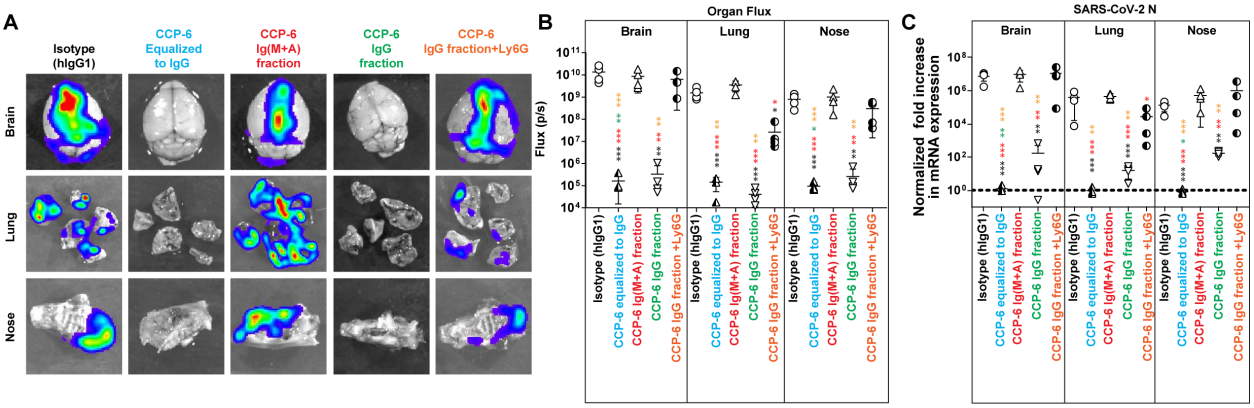

Figure S5 Neutrophils Contribute to Polyclonal IgG-mediated Protection During Prophylaxis in SARS-CoV-2-infected K18-hACE2 Mice. Related to Figure 5

(A-B) *Ex vivo* imaging of indicated organs and quantification of nLuc signal as flux(photons/sec) after necropsy for an experiment shown in Figure 5A

(C) Fold change in SARS-CoV-2 nucleocapsid (N gene) expression in brain, lung and nose tissues. The data were normalized to *Gapdh* mRNA expression in the same sample and that in non-infected mice after necropsy.

Grouped data in (B-C), were analyzed by 2-way ANOVA followed by Tukey's multiple comparison tests. Statistical significance for group comparisons to isotype control are shown in black, with IgG-equated CCP-6 are shown in cyan, with CCP-6/Ig(M+A) fraction are shown in red, with CCP-6/IgG fraction are shown in green and with CCP-6/IgG fraction under neutrophil depletion are shown in orange. $*$, $p < 0.05$; $**$, $p < 0.01$; $***$, $p < 0.001$; $****$, $p < 0.0001$; Mean values ± SD are depicted.

Figure S6

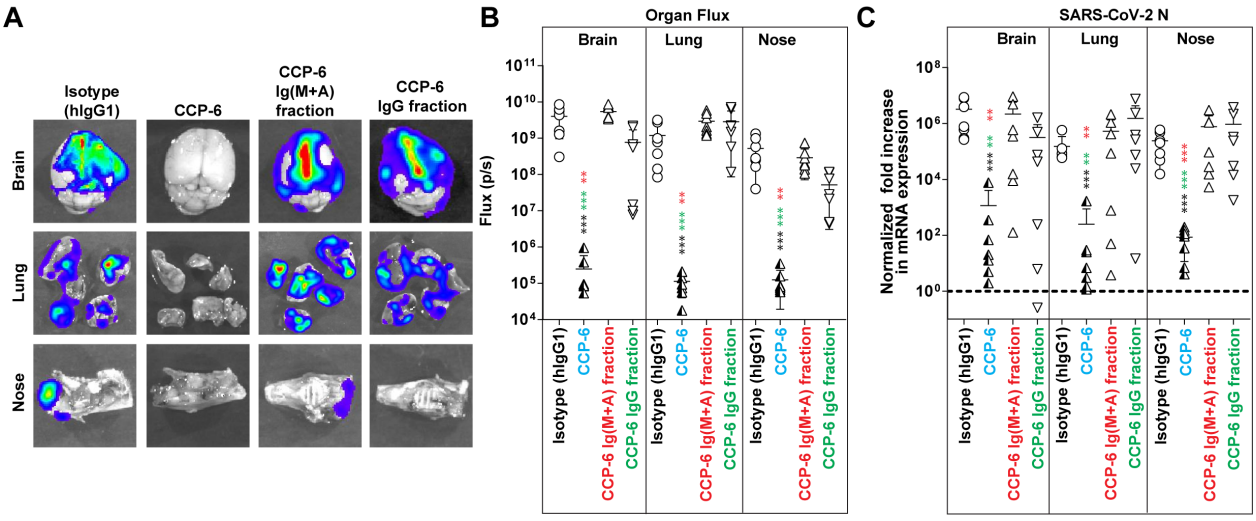

Figure S6. Polyclonal IgG and Ig(M+A) Contribute to Protection During CCP Therapy. Related to Figure 6

(A-B) *Ex vivo* imaging of indicated organs and quantification of nLuc signal as flux(photons/sec) after necropsy for an experiment shown in Figure 6A

(C) Fold change in SARS-CoV-2 nucleocapsid (N gene) expression in brain, lung and nose tissues. The data were normalized to *GAPDH* mRNA expression in the same sample and that in non-infected mice after necropsy.

Grouped data in (B-C), were analyzed by 2-way ANOVA followed by Tukey's multiple comparison tests. Statistical significance for group comparisons to isotype control are shown in black, with IgG-equated CCP-6 are shown in cyan, with CCP-6/Ig(M+A) fraction are shown in red, with CCP-6/IgG fractionare shown in green. ∗, $p < 0.05$; ∗∗, $p < 0.01$; ∗∗∗, $p < 0.001$; ∗∗∗∗, $p < 0.0001$; Mean values ± SD are depicted.

Table S1. Summary of in vivo efficacy analyses of CCPs in K18-hACE2 mice against SARS-CoV-2 WA1, Delta VOC and Beta VOC. Related to Figures 1-7

CCP	WA1				Delta				Beta			
	nAb (IC_{50})	ADCC (%)	Mortality		nAb (IC_{50})	ADCC (%)	Mortality		nAb (IC_{50})	ADCC (%)	Mortality	
			Prophylaxis	Therapy			Prophylaxis	Therapy			Prophylaxis	Therapy
CCP-2	3.5 (+/-)	1.30 Low	100% Death: 6 dpi	100% Death 6 dpi	5.4	0.60	100% Death: 6 dpi	100% Death: 6 dpi	9.5	0.00	100% Death: 6 dpi	100% Death: 6 dpi
CCP-3	1.37 (+)	16.17 Moderate	50% Delayed death: 9-12 dpi	75-100% Delayed death: 8 dpi	2.47	12.86	100% Delayed death: 8-11 dpi	100% Delayed death: 7-8 dpi	10.5	8.87	100% Delayed death: 7 dpi	100% Death: 6 dpi
			Post Innate cell dep 100% Delayed death: 6-7 dpi	Post Innate cell dep 100% Death: 6 dpi								
CCP-5	3.59 (+/-)	22.66 Moderate	50% Death: 10-12 dpi	75% Death: 8-12 dpi	12.29	17.48	75% Delayed death: 8-14 dpi	100% Delayed death: 7-8 dpi	10.8	13.98	100% Delayed death: 7-8 dpi	100% Death: 6 dpi
			Post innate cell dep 100% Delayed death: 6-7 dpi	Post innate cell dep 100% Death: 6 dpi								
CCP-6	0.6 (++)	40.62 High	0%	0%	0.55	26.13	50% Delayed death: 11-13 dpi	100% Delayed death: 9-10 dpi	2.12	19.72	100% Delayed Death: 8 dpi	100% Delayed death: 7 dpi
			Post innate cell dep 0%	Post innate cell dep 100% Delayed death: 6-7 dpi								